# On the Ergodic Capacity of NOMA-Based Cognitive Hybrid Satellite Terrestrial Networks

Xiaojuan Yan[1], Hailin Xiao[1,2], Cheng-Xiang Wang[3] and Kang An[4]
[1]School of Information and Communication, Guilin University of Electronic Technology, Guilin 541004, China.
[2]College of Physics and Electronic Information Engineering, Wenzhou University, Wenzhou 325035, China.
[3]Institute of Sensors, Signals and Systems, School of Engineering & Physical Sciences, Heriot-Watt University, Edinburgh, EH14 4AS, U.K.
[4]College of Communications Engineering, PLA University of Science and Technology, Nanjing 210007, China.
Email: yxj9609@163.com, xhl_xiaohailin@163.com, cheng-xiang.wang@hw.ac.uk, ankang@nuaa.edu.cn

***Abstract*—The cognitive hybrid satellite terrestrial networks (CHSTN) is regarded as an effective way to enhance the spectrum efficiency as well as mitigate the spectrum scarcity problem. In this paper, we introduce a non-orthogonal multiple access (NOMA) scheme, which has the ability to simultaneously serve multiple users, in the cognitive network to further improve the utilization of radio spectrum. With the help of Meijer-G functions, the analytical expression for ergodic capacity of the considered system is derived. Simulations are provided to show the advantage of introducing the NOMA scheme in the cognitive system and the effects of some parameters on the performance of the considered network.**

***Index Terms*—Cognitive hybrid satellite terrestrial networks, non-orthogonal multiple access scheme, ergodic capacity.**

## I. Introduction

CHSTN, in which a terrestrial network shares the spectrum with a satellite network by employing cognitive radio (CR) technology, has been proposed and viewed as an effective strategy to increase the spectrum efficiency and mitigate the problem of spectrum scarcity. Meanwhile, a significant number of works have been devoted to investigate the performance of CHSTN [1]–[6]. Assuming multiple antennas at the primary and secondary source, the work [1] investigated the ergodic capacity in a CHSTN. Considering the transmit power of secondary source was limited, the work [2] derived both exact closed-form and asymptotic expressions for outage probability (OP) of a CHSTN with the help of Meijer-G functions. In [3], the authors employed a multiple antennas relay in a downlink CHSTN to improve the OP performance. The authors in [4] studied two optimal power control schemes to maximize the delay-limited capacity and OP performance for CHSTN. Under the constraint of not deteriorating the communication of primary user, the authors in [5] and [6] investigated the optimal power allocation for secondary source in a downlink and uplink CHSTN, respectively.

Although these aforementioned works have investigated the performance measures such as OP and ergodic capacity for CHSTN, the key limitation of those prior studies is that they all provide service with orthogonal multiple access (OMA) scheme. Since only one user can be served at any time/frequency resource with OMA scheme, the limited time/spectrum resource in CHSTN is still underutilized. While high information transmission rate and large number of users are required in next generation network. Based on this observation, researchers have proposed a novel multiple access scheme, referred to as non-orthogonal multiple access (NOMA) scheme, which has the ability to superpose multiple signals in power domain and serve multiple users with the same time/frequency resource [7]. Several works have investigated the performance of NOMA scheme in a variety of different scenarios and proven that NOMA scheme could achieve a higher resource utilization [8]–[13]. In [8], the authors proposed a general power allocation which can guarantee the quality of services with NOMA scheme in uplink and downlink to outperform those with OMA scheme. The work [9] developed a new interfering channel alignment to deal with the inter-cell interference problem, which was caused by the biased power allocation strategy of NOMA scheme. The scenario of combining NOMA scheme and mmWave technology was studied in [10]. While an extension of [10] to a scenario which combined with NOMA scheme, multiple-input-multiple-output (MIMO), and mmWave technology was investigated in [11]. The authors in [12] introduced NOMA scheme in visible light communication multi-cell networks and proposed a user select strategy to mitigate interference. By assuming the user with better link quality as an energy harvesting relay, the work [13] investigated the OP and throughput performances of NOMA users with different user selection schemes in Rayleigh fading channels.

However, to the best of the authors' knowledge, most of the studies on NOMA application focus on terrestrial cellular network, no results regard to the application of NOMA scheme in CHSTN have been reported thus far. To fill this gap, in this paper, we consider a downlink CHSTN, where the NOMA scheme is employed to serve multiple secondary users simultaneously and further improve the efficiency of the limited resource in secondary network. Specifically, the ergodic capacity which is usefull in understanding the performance limits of the considered network is derived in terms of Meijer-G functions. Simulation results are provided to validate our theoretical formulas, show the superiority of introducing the NOMA scheme in the cognitive system, and the effects of various parameters on the system performance.

978-1-5386-4502-4/17/$31.00 ©2017 IEEE

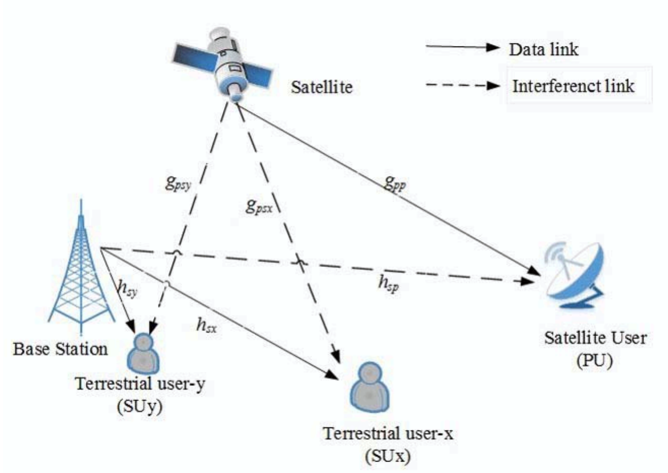


Fig. 1. Illustration of the system model.

## II. Signal Model

As illustrated in Fig. 1, we consider a CHSTN, where terrestrial network acting as a cognitive system shares the spectrum resource with satellite network which is the primary system. To further improve the spectrum utilization, NOMA scheme is adopted in terrestrial network. Due to the fact that the complexity of NOMA scheme with two users is the simplest, we assume two terrestrial users, i.e., user $y$ and user $x$, are selected to form a NOMA group for simplicity. Despite only two users are selected, we must highlight that the considered system can be easily extended to a more than two users scenario, and the difference is the power allocation factor at each user. Since our focus is on the superiority of introducing the NOMA scheme in the cognitive network, we assume that all nodes in Fig. 1 are equipped with a single antenna. Thus, the received signal at terrestrial users can be written as

$$y_m = h_{sm}x + \sqrt{P_{\rm p}}g_{{\rm ps}m}x_{\rm p} + n_m \tag{1}$$

where $h_{sm}$ and $g_{{\rm ps}m}$ ($m$=$x$, $y$) are the channel coefficients from the cognitive base station (BS) and satellite to terrestrial user $m$, respectively, $x = \sqrt{\alpha P_{\rm s}}x_y + \sqrt{(1-\alpha)P_{\rm s}}x_x$ denotes the superposing signal with $\alpha$ $(0 \le \alpha \le 1)$ representing the power allocation factor at user $y$, $P_{\rm s}$ being the transmit power at the terrestrial BS, and $x_m$ (E$\left[|x_m|^2\right] = 1$) denoting the transmit signal of user $m$, $P_{\rm p}$ is the transmit power at satellite, and $n_m$ denotes the additive white Gaussian noise (AWGN) at user $m$ with E$\left[|n_m|^2\right] = \delta^2$. To avoid the satellite user being interfered beyond an interference threshold $Q$, $P_{\rm s}$ should satisfy $P_{\rm s} = \frac{Q}{|h_{\rm sp}|^2}$ [1], where $h_{\rm sp}$ is the interference link from the terrestrial BS to satellite user.

Without loss of generality, We assume terrestrial users are ordered by their channel gain to interference plus noise ratios, i.e., $\frac{|h_{{\rm s}x}|^2}{P_{\rm p}|g_{{\rm ps}x}|^2+\delta^2} \le \frac{|h_{{\rm s}y}|^2}{P_{\rm p}|g_{{\rm ps}y}|^2+\delta^2}$. Thus, in the NOMA downlink, user $x$ decodes its signal directly and the end-to-end signal to interference plus noise ratio (SINR) of user $x$ can be given as

$$\gamma_x = \frac{(1-\alpha)P_{\rm s}|h_{{\rm s}x}|^2}{\alpha P_{\rm s}|h_{{\rm s}x}|^2 + P_{\rm p}|g_{{\rm ps}x}|^2 + \delta^2}. \tag{2}$$

While user $y$ first decodes and removes the signal of user $x$ based on the principle of successive interference cancellation (SIC), and the decoding SINR at user $y$ can be derived as

$$\gamma_{y\to x} = \frac{(1-\alpha)P_{\rm s}|h_{{\rm s}y}|^2}{\alpha P_{\rm s}|h_{{\rm s}y}|^2 + P_{\rm p}|g_{{\rm ps}y}|^2 + \delta^2}. \tag{3}$$

From (2) and (3), we can find that $\gamma_{y\to x} \ge \gamma_x$ since the assumption that a better channel gain to interference plus noise ratio is acquired at user $y$. In other words, the signal of user $x$ can be removed successfully at user $y$. In this regard, the SINR of user $y$ is

$$\gamma_y = \frac{\alpha P_{\rm s}|h_{{\rm s}y}|^2}{P_{\rm p}|g_{{\rm ps}y}|^2 + \delta^2}. \tag{4}$$

Before analyzing the ergodic capacity of the considered network, we first provide the statistical properties of the satellite and terrestrial channel links, which will be frequently invoked in next section.

Similar to [2]–[6], we assume the satellite links, i.e., $g_{\rm pp}$, $g_{{\rm ps}x}$, and $g_{{\rm ps}y}$, are following the independent and identically distributed (i.i.d.) Shadowed-Rician fading distribution, and the probability density function (PDF) of $|g_i|^2$ ($i$=ps$x$, ps$y$, pp) is given by [14], as

$$f_{|g_i|^2}(x) = \alpha_i e^{-\beta_i x}{}_1F_1(m_i;1;\delta_i x) \tag{5}$$

where $\alpha_i = 0.5(2b_im_i/(2b_im_i+\Omega_i))^{m_i}/b_i$, $\beta_i = 0.5/b_i$, $\delta_i = 0.5\Omega_i/b_i/(2b_im_i+\Omega_i)$, $2b_i$ is the average power of the scatter, $\Omega_i$ denotes the average power of line-of-sight component, $m_i$ $(m_i > 0)$ is the Nakagami-$m$ fading parameter, and ${}_1F_1(a;b;c)$ [15, Eq (9.100)] represents the confluent hypergeometric function. According to [5], the terrestrial links are modeled as i.i.d. Nakagami-m fading distribution, the PDF of $|h_j|^2$ ($j$=$h_{\rm sp}$, $h_{{\rm s}x}$, $h_{{\rm s}y}$) can be expressed as

$$f_{|h_j|^2}(y) = \frac{\xi_j^{m_j}y^{m_j-1}}{\Gamma(m_j)}e^{-\xi_j y} \tag{6}$$

where $\Gamma(\cdot)$ denotes the Gamma function, $\xi_j = m_j/\Omega_j$ with $m_j$ being the fading parameter and $\Omega_j$ the average power.

Further, based on (6) and the concept of conditional probability theory, we can derive the PDF of $f_{|h_{sm}|^2/|h_{\rm sp}|^2}(x)$ as

$$f_{|h_{sm}|^2/|h_{\rm sp}|^2}(x) = \int_0^\infty y f_{|h_{sm}|^2}(xy) f_{|h_{\rm sp}|^2}(y)dy. \tag{7}$$

With the help of [15, Eq.(3.351.3)], we get

$$f_{|h_{sm}|^2/|h_{\rm sp}|^2}(x) = \frac{\xi_{sm}^{m_{sm}}\xi_{\rm sp}^{m_{\rm sp}}x^{m_{sm}-1}\Gamma(m_{sm}+m_{\rm sp})}{\Gamma(m_{sm})\Gamma(m_{\rm sp})(\xi_{\rm sp}+\xi_{sm}x)^{m_{sm}+m_{\rm sp}}}. \tag{8}$$

## III. ERGODIC CAPACITY

The ergodic capacity is defined as the expected value of the instantaneous end-to-end mutual information [4], which can be expressed as

$$C_{\rm erg} = {\rm E}\left[\log_2\left(1+\gamma_x\right)\right] + {\rm E}\left[\log_2\left(1+\gamma_y\right)\right]. \tag{9}$$

By substituting (2) and (4) into (9) along with some simple mathematic manipulations, the ergodic capacity of the considered system in this paper can be derived as

$$\begin{aligned} C_{\rm erg} = \log_2(e)\,{\rm E}\Big\{&\ln\left(1+\overline{\gamma}_{\rm p}\left|g_{{\rm ps}x}\right|^2+\overline{\gamma}_{\rm Q}{\left|h_{{\rm s}x}\right|^2}\Big/{\left|h_{\rm sp}\right|^2}\right)\\ &-\ln\left(1+\overline{\gamma}_{\rm p}\left|g_{{\rm ps}x}\right|^2+\alpha\overline{\gamma}_{\rm Q}{\left|h_{{\rm s}x}\right|^2}\Big/{\left|h_{\rm sp}\right|^2}\right)\\ &+\ln\left(1+\overline{\gamma}_{\rm p}\left|g_{{\rm ps}y}\right|^2+\alpha\overline{\gamma}_{\rm Q}{\left|h_{\rm sy}\right|^2}\Big/{\left|h_{\rm sp}\right|^2}\right)\\ &-\ln\left(1+\overline{\gamma}_{\rm p}\left|g_{{\rm ps}y}\right|^2\right)\Big\} \end{aligned} \tag{10}$$

where $\overline{\gamma}_{\rm p} = {\rm E}[\gamma_{\rm p}] = {\rm E}[P_{\rm p}/\delta^2]$ is the average signal to noise ratio (SNR) at the satellite, and $\overline{\gamma}_{\rm Q} = {\rm E}[\gamma_{\rm Q}] = {\rm E}[Q/\delta^2]$ denotes the average SNR at the terrestrial BS, respectively. Unfortunately, the closed-form expression for the integration in (10) is mathematically intractable, we hereafter seek to consider the approximated expression of (10) in this paper. According to the result provided in [16], the analytical approximation of ${\rm E}\left(\ln\left(1+x\right)\right)$ can be obtained as

$${\rm E}\left(\ln\left(1+x\right)\right) \approx \ln\left(1+{\rm E}\left(x\right)\right) - \frac{{\rm E}\left(x^2\right)-\left({\rm E}\left(x\right)\right)^2}{2\left(1+{\rm E}\left(x\right)\right)^2}. \tag{11}$$

Based on (11), we start with the first summand in (10), which can be approximated as

$$\begin{aligned} &{\rm E}\left[\ln\left(1+\overline{\gamma}_{\rm p}\left|g_{{\rm ps}x}\right|^2+\overline{\gamma}_{\rm Q}{\left|h_{{\rm s}x}\right|^2}\Big/{\left|h_{\rm sp}\right|^2}\right)\right]\\ &\approx \ln\left(1+\overline{\gamma}_{\rm p}{\rm E}\left(\left|g_{{\rm ps}x}\right|^2\right)+\overline{\gamma}_{\rm Q}{\rm E}\left({\left|h_{{\rm s}x}\right|^2}\Big/{\left|h_{\rm sp}\right|^2}\right)\right)\\ &+\frac{\left(\overline{\gamma}_{\rm p}{\rm E}\left(\left|g_{{\rm ps}x}\right|^2\right)+\overline{\gamma}_{\rm Q}{\rm E}\left({\left|h_{{\rm s}x}\right|^2}\Big/{\left|h_{\rm sp}\right|^2}\right)\right)^2}{2\left(1+\overline{\gamma}_{\rm p}{\rm E}\left(\left|g_{{\rm ps}x}\right|^2\right)+\overline{\gamma}_{\rm Q}{\rm E}\left({\left|h_{{\rm s}x}\right|^2}\Big/{\left|h_{\rm sp}\right|^2}\right)\right)^2}\\ &-\frac{\overline{\gamma}_{\rm p}^2{\rm E}\left[\left(\left|g_{{\rm ps}x}\right|^2\right)^2\right]+\overline{\gamma}_{\rm Q}^2{\rm E}\left[\left({\left|h_{{\rm s}x}\right|^2}\Big/{\left|h_{\rm sp}\right|^2}\right)^2\right]}{2\left(1+\overline{\gamma}_{\rm p}{\rm E}\left(\left|g_{{\rm ps}x}\right|^2\right)+\overline{\gamma}_{\rm Q}{\rm E}\left({\left|h_{{\rm s}x}\right|^2}\Big/{\left|h_{\rm sp}\right|^2}\right)\right)^2}\\ &-\frac{\overline{\gamma}_{\rm p}\overline{\gamma}_{\rm s}{\rm E}\left(\left|g_{{\rm ps}x}\right|^2\right)\overline{\gamma}_{\rm Q}{\rm E}\left({\left|h_{{\rm s}x}\right|^2}\Big/{\left|h_{\rm sp}\right|^2}\right)}{\left(1+\overline{\gamma}_{\rm p}{\rm E}\left(\left|g_{{\rm ps}x}\right|^2\right)+\overline{\gamma}_{\rm Q}{\rm E}\left({\left|h_{{\rm s}x}\right|^2}\Big/{\left|h_{\rm sp}\right|^2}\right)\right)^2}. \end{aligned} \tag{12}$$

In order to compute (12), we first compute the $n^{th}$-order moments of $\left|g_{{\rm ps}x}\right|^2$ as

$${\rm E}\left[\left|g_{{\rm ps}x}\right|^{2n}\right] = \int_0^\infty y^n f_{\left|g_{{\rm ps}x}\right|^2}\left(y\right)dy. \tag{13}$$

Substituting (5) into (13) and expanding ${}_1F_1\left(m_{{\rm ps}x};1;\delta_{{\rm ps}x}y\right)$ in Meijer-G functions via [15, Eq. (8.455.1)], as

$${}_1F_1\left(m_{{\rm ps}x};1;\delta_{{\rm ps}x}y\right)=\frac{1}{\Gamma\left(m_{{\rm ps}x}\right)}G_{1,2}^{1,1}\left[-\delta_{{\rm ps}x}y\left|\begin{matrix}1-m_{{\rm ps}x}\\0,0\end{matrix}\right.\right] \tag{14}$$

where $G_{1,2}^{1,1}\left[\cdot\right]$ [15, Eq. (9.301)] is the Meijer-G functions with one variable. Then, with the aid of [15, Eq. (7.813.1)], we get

$${\rm E}\left[\left|g_{{\rm ps}x}\right|^{2n}\right]=\frac{\alpha_{{\rm ps}x}}{\Gamma\left(m_{{\rm ps}x}\right)\beta_{{\rm ps}x}^{n+1}}G_{2,2}^{1,2}\left[\frac{-\delta_{{\rm ps}x}}{\beta_{{\rm ps}x}}\left|\begin{matrix}-n,1-m_{{\rm ps}x}\\0,0\end{matrix}\right.\right]. \tag{15}$$

The $n^{th}$-order moments of ${\left|h_{{\rm s}x}\right|^2}\Big/{\left|h_{\rm sp}\right|^2}$ can be derived as

$$\begin{aligned} &{\rm E}\left[\left({\left|h_{{\rm s}x}\right|^2}\Big/{\left|h_{\rm sp}\right|^2}\right)^n\right]\\ &= \Xi_{{\rm s}x}\int_0^\infty y^{m_{{\rm s}x}+n-1}\left(1+\xi_{{\rm s}x}y/\xi_{\rm sp}\right)^{-m_{{\rm s}x}-m_{\rm sp}}dy \end{aligned} \tag{16}$$

with

$$\Xi_{{\rm s}x} = \frac{\xi_{{\rm s}x}^{m_{{\rm s}x}}\Gamma\left(m_{{\rm s}x}+m_{\rm sp}\right)}{\Gamma\left(m_{{\rm s}x}\right)\Gamma\left(m_{\rm sp}\right)\xi_{\rm sp}^{m_{{\rm s}x}}}. \tag{17}$$

Using the identity [17, Eq. (10)], we can get

$$\begin{aligned} \left(1+\xi_{{\rm s}x}y/\xi_{\rm sp}\right)^{-m_{{\rm s}x}-m_{\rm sp}} &= \frac{1}{\Gamma\left(m_{{\rm s}x}+m_{\rm sp}\right)}\\ \times G_{1,1}^{1,1}&\left[\frac{\xi_{{\rm s}x}y}{\xi_{\rm sp}}\left|\begin{matrix}1-m_{{\rm s}x}-m_{\rm sp}\\0\end{matrix}\right.\right] \end{aligned} \tag{18}$$

Substituting (18) into (16) along with the help of [15, Eq. (7.811.4)], we get

$${\rm E}\left[\left({\left|h_{{\rm s}x}\right|^2}\Big/{\left|h_{\rm sp}\right|^2}\right)^n\right] = \frac{\xi_{\rm sp}^n/\xi_{{\rm s}x}^n\Gamma\left(m_{{\rm s}x}+n\right)\Gamma\left(m_{\rm sp}-n\right)}{\Gamma\left(m_{{\rm s}x}\right)\Gamma\left(m_{\rm sp}\right)}. \tag{19}$$

To this end, Eq. (12) can be calculated with $n$=1, 2.

Due to the fact that $\left|g_{{\rm ps}y}\right|^2$ and $\left|h_{{\rm s}y}\right|^2$ have the same PDF form with $\left|g_{{\rm ps}x}\right|^2$ and $\left|h_{{\rm s}x}\right|^2$, respectively. We can compute the second and third commands of (10) by following the similar steps of deriving (12). Then, the remaining task is to compute the forth term in (10), by using [17, Eq. (11)], $\ln\left(1+y\right)$ can be written as

$$\ln\left(1+y\right) = G_{2,2}^{1,2}\left[y\left|\begin{matrix}1,1\\1,0\end{matrix}\right.\right]. \tag{20}$$

Using (5) and (20) conjunction with the help of [18, Eq. (2.6.2)], the forth command of (10) can be obtained as

$$\begin{aligned} {\rm E}\left[\ln\left(1+\overline{\gamma}_{\rm p}\left|g_{{\rm ps}y}\right|^2\right)\right] &= \frac{\alpha_{{\rm ps}y}}{\Gamma\left(m_{{\rm ps}y}\right)\beta_{{\rm ps}y}}\\ \times G_{1,[2:1],0,[2:2]}^{1,2,1,1,1}&\left[\begin{matrix}\frac{\overline{\gamma}_{\rm p}}{\beta_{{\rm ps}y}}\\ \frac{-\delta_{{\rm ps}y}}{\beta_{{\rm ps}y}}\end{matrix}\left|\begin{matrix}1,1\\1,1;1-m_{{\rm ps}y}\\--\\1,0;0,0\end{matrix}\right.\right]. \end{aligned} \tag{21}$$

where $G_{1,[2:1],0,[2:2]}^{1,2,1,1,1}\left[\cdot\right]$ [18] is the generalized Meijer-G functions with two variables, which can be computed with the method proposed in [19].

Finally, pulling everything together, the asymptotic result for the ergodic capacity of the considered system can be obtained.

TABLE I
SATELLITE CHANNEL PARAMETERS [14].

| Shadowing | $b_i$ | $m_i$ | $\Omega_i$ |
|---|---|---|---|
| Heavy shadowing (HS) | 0.063 | 0.739 | $8.97 \times 10^{-4}$ |
| Average shadowing (AS) | 0.126 | 10.1 | 0.835 |
| Light shadowing (LS) | 0.158 | 19.4 | 1.29 |

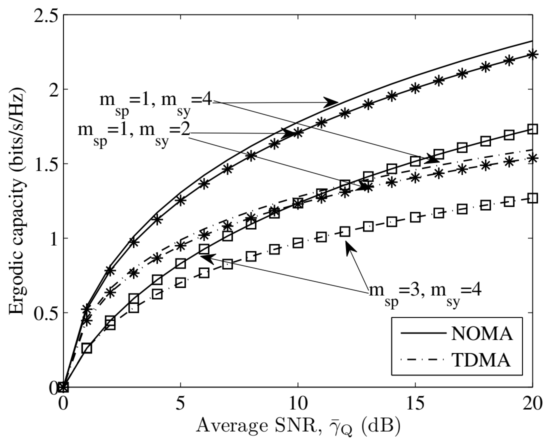


Fig. 2. The ergodic capacity versus $\bar{\gamma}_Q$ for various terrestrial channel parameters.

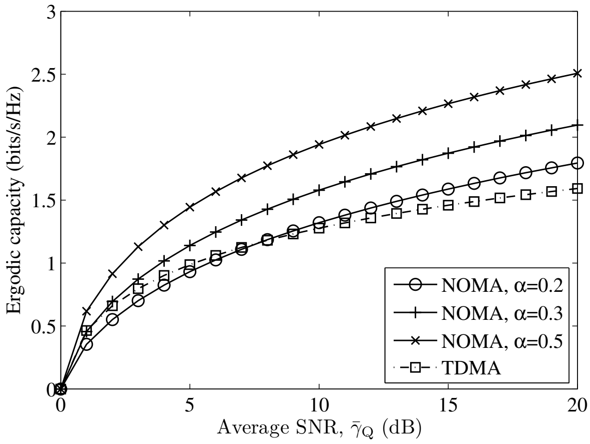


Fig. 3. The ergodic capacity versus $\bar{\gamma}_Q$ for various power allocation coefficient $\alpha$.

## IV. SIMULATION RESULTS AND ANALYSIS

In this section, simulation results are provided to show the validity of our theoretical analysis, the superiority of the proposed NOMA-based strategy in CHSTN. In the simulations, according to [14], the satellite channel parameters are provided in Table I. In addition, because the range of terrestrial network is much smaller than that of the satellite network, we assume the links between satellite to terrestrial users undergo the same fading and set $|g_{psx}|^2 = |g_{psy}|^2$. Moreover, based on the power allocation principle of NOMA scheme, the user with worse channel gain can be allocated more power, thus in this paper we consider $\alpha \leq 0.5$. The TDMA scheme which transmits data in two orthogonal time slots is given for comparison in all cases.

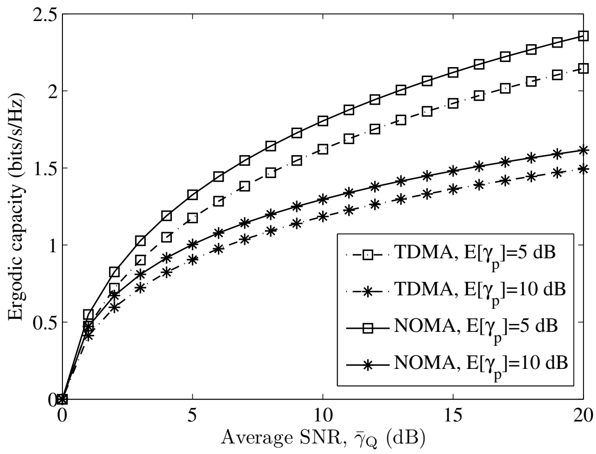


Fig. 4. The ergodic capacity versus $\bar{\gamma}_Q$ for different $\mathrm{E}[\gamma_p]$.

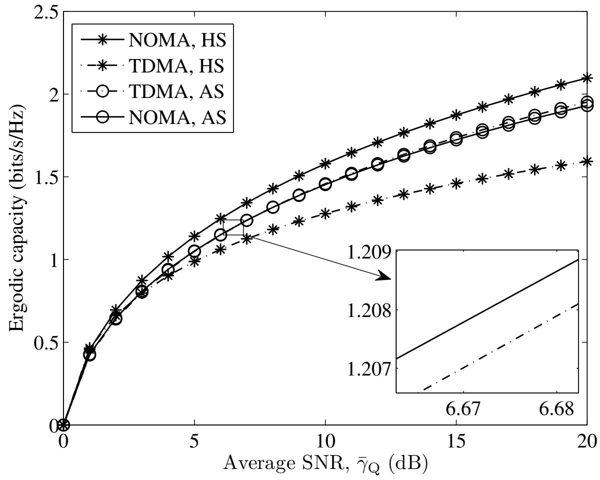


Fig. 5. The ergodic capacity versus $\bar{\gamma}_Q$ for different satellite link configurations.

Fig. 2 shows the comparison of ergodic capacity with NOMA and TDMA schemes for different terrestrial channel parameters, where we consider the power allocation coefficient $\alpha = 0.4$, $m_{sx} = 1$, and $\bar{\gamma}_p = 5$ dB for heavy shadowing. As we see, the ergodic capacity curves with NOMA scheme are superior to those with the TDMA scheme, particularly at high $\bar{\gamma}_Q$. This phenomenon indicates that higher ergodic capacity and resource utilization with the NOMA scheme can be achieved with the same amount of transmit power at terrestrial BS. Moreover, we can note that the ergodic capacity performance degrades when either the link parameter $m_{sy}$ decreases or the parameter $m_{sp}$ increases. This is an expected result because a smaller $m_{sy}$ corresponds to a worse propagation condition between the cognitive BS and user $y$, while a bigger $m_{sp}$ corresponds to a lower transmit power at cognitive BS for the protection of the satellite user.

Fig. 3 depicts the effect of different power allocation coefficient $\alpha$ on the ergodic capacity performance by considering $\bar{\gamma}_{\rm p} = 5$ dB, $m_{\rm sp} = m_{\rm sx} = 1$, and $m_{\rm sy} = 4$ for heavy shadowing. It can be found that as the power allocation factor $\alpha$ decreases, the ergodic capacity of the considered network degrades. This is because lower power allocation factor means that the user with better channel gain to interference plus noise ratio is allocated with less power. Specially, when $\alpha = 0.2$, the ergodic capacity with the NOMA scheme at low $\bar{\gamma}_{\rm Q}$ is inferior to that with the TDMA scheme, implying that the ergodic capacity with a fixed power allocation NOMA scheme can not outperform that with the TDMA scheme in certain case, we should provide a flexible power allocation strategy to assure the superiority of applying the NOMA scheme in CHSTN.

Fig. 4 illustrates the impact of different $\bar{\gamma}_{\rm p}$ on the ergodic capacity of the considered system, where $\alpha = 0.4$, $m_{\rm sx} = 3$, and $m_{\rm sy} = 6$ for heavy shadowing are considered. It can be seen that an increase in $\bar{\gamma}_{\rm p}$ can cause significantly degradation of the capacity performance, since the interference from primary network becomes stronger. However, the ergodic capacity with the NOMA scheme outperform the TDMA scheme in all cases.

Fig. 5 plots the ergodic capacity curves for various satellite link configurations, where we consider $\alpha = 0.3$, $m_{\rm sx} = m_{\rm sp} = 1$, $m_{\rm sy} = 4$, and $\bar{\gamma}_{\rm p} = 5$ dB. As observed, the superiority of ergodic capacity with the NOMA scheme under average shadowing is inferior to that under heavy shadowing. This phenomenon suggests that we should take the effect of satellite channel configurations into account when setting the power allocation strategy.

## V. Conclusions

In this paper, we have investigated the ergodic capacity of a downlink CHSTN with a NOMA scheme. Considering the limited transmit power at the terrestrial BS, we have derived a theoretical expression for the ergodic capacity of the considered system. Simulation results have provided to show the superiority of introducing the NOMA scheme in CHSTN, the impact of key parameters such as terrestrial and satellite channel parameters, power allocation coefficient, and different transmit power on system performance. Our findings have illustrated that a higher ergodic capacity and resource utilization can be achieved with the NOMA scheme in most cases, but the NOMA scheme with fixed power allocation strategy is inferior to the TDMA scheme in some cases. Thus, a flexible power allocation scheme taking into account various parameters such as the satellite fading severity, the terrestrial link quality, and the available power at terrestrial BS should be considered when performing NOMA scheme in CHSTN.

## Acknowledgment

The authors gratefully acknowledge the support from the EU H2020 RISE TESTBED project (No. 734325), EU FP7 QUICK project (No. PIRSES-GA-2013-612652), EPSRC TOUCAN project (No. EP/L020009/1), Innovation Project of Guangxi Graduate Education, and Innovation Project of GUET Graduate Education (No. 2016YJCXB05).

## References

[1] K. An, M. Lin, T. Liang, J. Ouyang, and W.-P. Zhu, "On the ergodic capacity of multiple antenna cognitive satellite terrestrial networks," in *Proc. IEEE ICC'16*, Kuala Lumpur, Malaysia, July. 2016.

[2] K. An, M. Lin, W.-P. Zhu, Y. Huang, and G. Zheng, "Outage performance of cognitive hybrid satellite-terrestrial networks with interference constraint," *IEEE Trans. Veh. Technol.*, vol. 65, no. 11, pp. 9397–9404, Nov. 2016.

[3] K. An, J. Ouyang, M. Lin, and T. Liang, "Outage analysis of multi-antenna cognitive hybrid satellite-terrestrial relay networks with beamforming," *IEEE Commun. Lett.*, vol. 19, no. 7, pp. 1157–1160, July. 2015.

[4] S. Shi, G. Li, K. An, Z. Li, and G. Zheng, "Optimal power control for real-time applications in cognitive satellite terrestrial networks," *IEEE Commun. Lett.*, in press.

[5] S. Vassaki, M. I. Poulakis, A. D. Panagopoulos, and P. Constantinou, "Power allocation in cognitive satellite terrestrial networks with QoS constraints," *IEEE Commun. Lett.*, vol. 17, no. 7, pp. 1344–1347, July. 2013.

[6] S. Vassaki, M. I. Poulakis, and A. D. Panagopoulos, "Optimal iSINR-based power control for cognitive satellite terrestrial networks," *Wiley Trans. Emerging Tel. Tech.*, vol. 28, no. 2, Feb. 2017.

[7] Y. Saito, Y. Kishiyama, A. Benjebbour, T. Nakamura, A. Li, and K. Higuchi, "Non-orthogonal multiple access (NOMA) for cellular future radio access," in *Proc. VTC'13*, Dresden, Germany, Jun. 2013, pp. 1–5.

[8] Z. Yang, Z. Ding, P. Fan, and N. Al-Dhahir, "A general power allocation scheme to guarantee quality of service in downlink and uplink NOMA systems." *IEEE Trans. Wireless Commun.*, vol. 15, no. 11, pp. 7244–7257, Nov. 2016.

[9] W. Shin, M. Vaezi, J. Lee, and H. V. Poor, "On the number of users served in MIMO-NOMA cellular networks." in *Proc. ISWCS'16*, Poznan, Poland, Sept. 2016, pp. 638–642.

[10] S. A. R. Naqvi and S. A. Hassan, "Combining NOMA and mmWave technology for cellular communication." in *Proc. VTC'16*, Montreal, QC, Canada, Sept. 2016.

[11] D. Zhang, Z. Zhou, C. Xu, Y, Zhang. J. Rodriguez, and Takuro Sato, "Capacity analysis of non-orthogonal multiple access with mmWave massive MIMO systems." *IEEE J. Sel. Areas Commun.*, in press.

[12] X. Zhang, Q. Gao, C. Gong, and Z. Xu, "User grouping and power allocation for NOMA visible light communication multi-cell networks." *IEEE Commun. Lett.*, vol. 21, no. 4, pp. 777–780, Apr. 2017.

[13] Y. Liu, Z. Ding, M. Elkashlan, and H. V. Poor, "Cooperative non-orthogonal multiple access with simultaneous wireless information and power transfer," *IEEE J. Sel. Areas Commun.*, vol. 34, no. 4, pp. 938–953, Apr. 2016.

[14] A. Abdi, W. Lau, M.-S. Alouini, and M. Kaveh, "A new simple model for land mobile satellite channels: first and second order statistics," *IEEE Trans. Wireless. Commun.*, vol. 2, no. 3, pp. 519–528, May 2003.

[15] I. S. Gradshteyn and I. M. Ryzhik, *Table of Integrals, Series, and Products*, 7th ed. New York, NY, USA: Academic, 2007.

[16] Y. Huang, F. Al-Qahtani, C. Zhong, Q. Wu, J. Wang, and H. Alnuweiri, "Performance analysis of multiuser multiple antenna relaying networks with co-channel interference and feedback delay," *IEEE Trans. Commun.*, vol. 62, no. 1, pp. 59–73, Jan. 2014.

[17] V. S. Adamchik and O. I. Marichev, "The algorithm for calculating integrals of hypergeometric type functions and its realization in reduce systems," in *Proc. ISSAC'90*, Tokyo, Japan, Aug. 1990, pp. 212–224.

[18] A. M. Mathai and R. K. Saxena, *The H-function with applications in statistics and other disciplines*, New York, NY, USA:Wiley, 1978.

[19] R. P. Agrawal, "On certain transformation formulae and Meijer's G-function of two variables," *Indian J. Pure Appl. Math.*, vol. 1, no. 4, pp. 537–551, Mar. 1970.